Nanogel-Based Filler-Matrix Interphase for Polymerization Stress Reduction

B.M. Fronza[1] ![ORCID], I.Y. Rad[2], P.K. Shah[3] ![ORCID], M.D. Barros[2], M. Giannini[1], and J.W. Stansbury[2,3]

Abstract

A novel filler-resin matrix interphase structure was developed and evaluated for dental composite restoratives. Nanogel additives were chemically attached to the filler surface to use this created interphase as a potential source of compliance to minimize stress development during polymerization. In addition, we evaluated the effects of free nanogel dispersion into the resin matrix, combined or not with nanogel-modified fillers. Nanogels with varied characteristics were synthesized (i.e., size, 5 and 11 nm; glass transition temperature, 28 °C to 65 °C). Glass fillers were treated with trimethoxyvinylsilane and further reacted with thiol-functionalized nanogels via a free radical thiol-ene reaction. γ-Methacryloxypropyltrimethoxysilane-surface treated fillers were used as a control. Composites were formulated with BisGMA/TEGDMA resin blend with 60 wt% fillers with nanogel-modified fillers and/or free nanogel additives at 15 wt% in the resin phase. Polymerization kinetics, polymerization stress, volumetric shrinkage, and rheological and mechanical properties were evaluated to provide comprehensive characterization. Nanogel-modified fillers significantly reduced the polymerization stress from 2.2 MPa to 1.7 to 1.4 MPa, resulting in 20% stress reduction. A significantly greater nanogel content was required to generate the same magnitude stress reduction when the nanogels were dispersed only in the resin phase. When the nanogel-modified filler surface treatment and resin-dispersed nanogel strategies were combined, there was a stress reduction of 50% (values of 1.2 to 1.1 MPa). Polymerization rate and volumetric shrinkage were significantly reduced for systems with nanogel additives into the resin. Notably, the flexural modulus of the materials was not compromised, although a slight reduction in flexural strength associated with the nanogel-modified interphase was observed. Overall, modest amounts of free nanogel additives in the resin phase can be effectively combined with a limited nanogel content filler-resin interphase to lower volumetric shrinkage and dramatically reduce overall polymerization stress of composites.

Keywords: polymers, methacrylates, silanes, photopolymerization, dental composites, interface

Introduction

Polymerization stress (PS) in dental composites can damage the resin-tooth bonded interface, exhibiting a positive correlation with gap formation and leakage of restorations (Boaro et al. 2014; Fronza et al. 2015). It can also lead to cuspal deflection, tooth cracking, reduced bond strength, and lowered mechanical properties of the restorative material (Nayif et al. 2008; Braga et al. 2013). During polymerization, postgel stress buildup begins with the evolution of elastic modulus with the degree to which polymerization shrinkage is constrained by bonding to substrates (Braga et al. 2005). Free shrinkage is determined by the initial reactive group density within the resin and the degree of conversion (DC) attained, while elastic modulus (EM) is a function of polymer network density and increasing glass transition temperature (Tg) as polymerization occurs (Stansbury 2012). Addition of fillers to the resin affects both parameters. Increased filler volume fraction accounts for a reduction in the overall resin reactive group concentration, which reduces bulk shrinkage; however, increased filler loading also produces a significant increase in elastic modulus that can counter the stress reduction of lower shrinkage (Shah and Stansbury 2014).

γ-Methacryloxypropyltrimethoxysilane (MPS) is commonly used to provide a covalent linkage between fillers and resin matrix, which increases bulk mechanical properties through transfer of stresses between the inorganic and organic phases (Wilson et al. 2007). Despite the reactive methacrylate functional groups from the silane being relatively immobile and buried, which leads to inefficient coupling between phases, the resin-filler interface contributes to the buildup of significant internal stresses in composites during polymerization (Soderholm 1984; Sideridou and Karabela 2009).

Most advances to reduce PS focus on modification of the polymeric network, such as the use of step-growth thiol-Michael polymerizations. Nevertheless, further investigations are needed to achieve optimal proportions of resin, fillers, and

[1]Restorative Dentistry Department, Piracicaba Dental School, University of Campinas, Piracicaba, SP, Brazil
[2]Craniofacial Biology Department, University of Colorado, Aurora, CO, USA
[3]Chemical and Biological Engineering, University of Colorado, Boulder, CO, USA

A supplemental appendix to this article is available online.

Corresponding Author:
J.W. Stansbury, University of Colorado Anschutz Medical Campus, 12800 E 19th Ave, MS 8310, Aurora, CO 80045, USA.
Email: jeffrey.stansbury@ucdenver.edu

Table 1. Gel Permeation Chromatography Parameters, Glass Transition Temperature, and SH Content from Ellman's Reagent Test.

Nanogel	Composition	M_n, kg/mol	PDI	Rh, nm	Tg, °C	SH, mMol/g
1	IBMA/UDMA 70:30: 15 mol% ME + 10 mol% PETMP	17.8	1.1	2.5	49	0.09
2	IBMA/UDMA 70:30: 5 mol% ME + 10 mol% PETMP	182.3	5.4	5.8	65	0.08
3	BMA/UDMA 70:30: 15 mol% ME + 10 mol% PETMP	19.3	1.4	2.6	28	0.13

Data represent single analyses.
IBMA, isobornyl methacrylate; ME, 2-mercaptoethanol; M_n, number-average molecular weight; PDI, polydispersity index; PETMP, pentaerythritol tetra(3-mercaptopropionate); Rh, hydrodynamic radius; SH, thiol content per gram of nanogel; Tg, glass transition temperature; UDMA, urethane dimethacrylate.

photobase initiators to suit clinical use (Huang et al. 2018). Dimethacrylate monomers containing linkages capable of addition-fragmentation chain transfer behavior during polymerization also reduce stress; however, at elevated concentrations, this can compromise reactivity, conversion, and mechanical properties (Shah et al. 2017). Although advantages of chain transfer reactions with thiols (Pfeifer et al. 2011) or methacrylate-thiol-ene systems (Boulden et al. 2011) are promising to lower PS, use of small molecule thiols is usually related to reduced shelf life and unpleasant odor prior to polymerization. These drawbacks can be overcome with oligomeric thiols, such as off-stoichiometric thiourethanes (Bacchi et al. 2016; Bacchi et al. 2018); nonetheless, its effect to lower PS is concentration dependent, in which higher amounts increase resin viscosity, impairing addition of fillers and conceding handling characteristics. Recently, use of a thiourethane-modified silane was demonstrated to reduce the PS of composites as well (Faria et al. 2018).

Another alternative to reduce shrinkage and PS involves reactive nanogels (Moraes et al. 2011; Liu et al. 2012). Nanogels are highly tailorable polymeric particles that are attractive for biomedical applications, such as drug delivery systems and tissue engineering (Jiang et al. 2014; Zhang et al. 2016). Nanogels are physical or covalent network polymers that can be varied in size, character (i.e., Tg, refractive index, hydrophobicity), and functionality. Nanogel addition potentially provides enhanced polymerization rates with increased limiting conversion while significantly reducing the rate and extent of PS (Dailing et al. 2013). Reactive nanogel addition to resin and composites has been demonstrated to reduce stress without compromise to mechanical properties. However, nanogel dispersion into resin can increase resin viscosity and composite paste consistency (Moraes et al. 2011).

To overcome these issues, we developed a novel interphase structure between fillers and resin matrix based on minimal amounts of nanogel additives located at the filler surface, to use this interphase as a source of compliance to minimize stress development during polymerization. This concept relies on small relaxation potential designed into the interphase region that offers the prospect for substantial bulk stress reduction based on the high overall interfacial surface area present in highly filled composite materials. In this way, the utility of the interface extends beyond just a connection between phases.

Therefore, the objective of this study was to treat filler surfaces with systematically varied nanogels to reduce PS of restorative composites. In addition, we evaluated the physicochemical property effects when free nanogel was included in the resin matrix in combination with nanogel-modified fillers. The hypotheses tested were as follows: 1) nanogel-modified fillers will reduce the PS of composites, and 2) there will be no compromise to modulus of composites relative to control materials.

Materials and Methods

Nanogel Syntheses

Three nanogels with different sizes and Tg's were prepared (Table 1). Nanogels 1 and 2 were synthesized from isobornyl methacrylate and urethane dimethacrylate at a 70:30 molar ratio. To avoid macrogelation and to control nanogel molecular weight/particle size, nanogel 1 (Ng 1) used 15 mol% of a chain transfer agent (2-mercaptoethanol; ME) and 6-fold excess of solvent (methyl ethyl ketone; MEK), while Ng 2 used 5 mol% ME and 4-fold excess of MEK. To provide a lower Tg, Ng 3 was synthesized with butyl methacrylate, replacing isobornyl methacrylate, and with 15 mol% ME with a 6-fold excess of MEK. Azobisisobutyronitrile (1 wt%) was used as a thermal initiator. Free radical polymerization was carried out in solution at 80 °C (200-rpm stirring rate). Methacrylate conversion during nanogel synthesis was followed (C=C peak area at 1,637 cm^{-1} relative to C=O absorbance at 1,720 cm^{-1}) in mid-infrared spectra (Nicolet 6700; Thermo Scientific). At 60% conversion, pentaerythritol tetra(3-mercaptopropionate) (10 mol%) was added to introduce pendant thiol functionalities in the nanogels as the reaction progressed until 85% conversion. Nanogels were precipitated by dropwise addition into hexanes (10-fold excess). Residual solvent was removed, and nanogels were obtained as powders.

Isolated nanogels were characterized by triple-detector gel permeation chromatography; nanogel Tg was determined by dynamic mechanical analysis; and Ellman's reagent test was used to quantify free sulfhydryl groups on nanogels. Detailed methodologies are described in the Appendix.

Filler Surface Treatment

To introduce thiol-functionalized nanogels to the surface of a bare barium glass filler (mean diameter, 1 μm; Dentsply Sirona), the filler was initially treated with trimethoxyvinylsilane (VIN). A separate control filler was prepared by analogous surface treatment with MPS. Silanization methods are described in the Appendix.

Pendant vinyl groups from VIN on the filler surface were reacted with nanogels via a free radical thiol-ene reaction (Lowe 2010). The reaction was carried out with a filler:nanogel weight ratio of 1:3 in toluene at 70 °C and a stirring rate of 200 rpm for 48 h, with 1 wt% azobisisobutyronitrile added at the beginning of the reaction and again after 24 h. The reaction time was determined by a pilot study in which times of 24, 48, and 72 h were tested regarding the extent of nanogel attachment in coordination with composite property testing (see Appendix). Multistep solvent washing of the treated fillers with acetone was performed to remove any unbound nanogel, which was then followed by solvent removal during 24-h vacuum storage.

Filler treatments were analyzed by diffuse reflectance Fourier transform infrared spectroscopy, thermogravimetric analysis, and energy-dispersive x-ray spectrometry analysis, as described in the Appendix. Filler surface images were obtained by transmission electron microscopy (JEM 2100; JEOL).

Figure 1. Thermogravimetric analysis displays filler surface coverage with silane (1 wt%) in relation to the nontreated filler and added nanogels (3 ± 1 wt%). (**A**) The major weight loss associated with nanogel treatment starts around 250 °C, which, with the mass loss, confirms that nanogels are reacted to the surface. Diffuse reflectance spectroscopy shows free silanol groups (3,742 cm^{-1}; arrow) for untreated glass fillers, which were consumed after silanization. Methacrylate carbonyl peak at 1,706 cm^{-1} (asterisk) is present for γ-methacryloxypropyltrimethoxysilane and in a higher intensity for nanogel treatments. (**B**) Multiple aliphatic peaks (2,856 to 2,962 cm^{-1}) can also be observed for nanogel treatments. (**C**, **D**) Energy-dispersive x-ray spectrometry analysis identified C, O, Al, Si, and Ba in silanated fillers composition. (**E**) Elemental mapping demonstrates uniform distribution of S on the filler surface, correspondent to thiol-functional groups on the surface-bound nanogels. The filler surface can be observed in a transmission electron microscopy image with no treatment (300,000×, **F**) and with nanogel attachment found both isolated and in agglomerates (300,000×, **G**), with size compatible to gel permeation chromatography characterization (VIN Ng 2 at 500,000×, **H**). Ng, nanogel; VIN, trimethoxyvinylsilane.

Resin and Composite Formulation

A resin blend was formulated with bisphenol A glycidyl dimethacrylate (BisGMA; Esstech) and triethylene glycol dimethacrylate (TEGDMA; Esstech) in a 70:30 molar ratio. The visible light photoinitiator system consisted of camphorquinone (0.3 wt%; Sigma Aldrich) and ethyl 4-dimethylaminobenzoate (0.8 wt%; Sigma Aldrich). Fillers were mechanically mixed into the resins (5 min at 2,000 rpm; DAC 150 Speed Mixer, Flacktek). Besides the nanogel-functionalized fillers, the different nanogels were also tested as free additives in the resin. In this way, 4 sets of materials were formulated and tested: resin systems containing 15 wt% of free nanogel additives, composites with 60 wt% MPS fillers and 15 wt% of nanogel additives, composites with 60 wt% VIN nanogel-functionalized fillers, and composites with 60 wt% VIN nanogel-functionalized fillers combined with 15 wt% of nanogel additives.

Resin and Composites Testing

Real-time polymerization kinetics was monitored by Fourier transform near-infrared spectroscopy (Nicolet 6700; detailed settings described in the Appendix). Specimens (n = 3; 6 mm in diameter and 0.8-mm-thick discs) were light activated for 20 s at an incident irradiance of 1,470 mW/cm^2 at 430- to 480-nm wavelength (Elipar DeepCure-S LED; 3M ESPE). Measurements were taken to assess DC and provide the dynamic polymeriza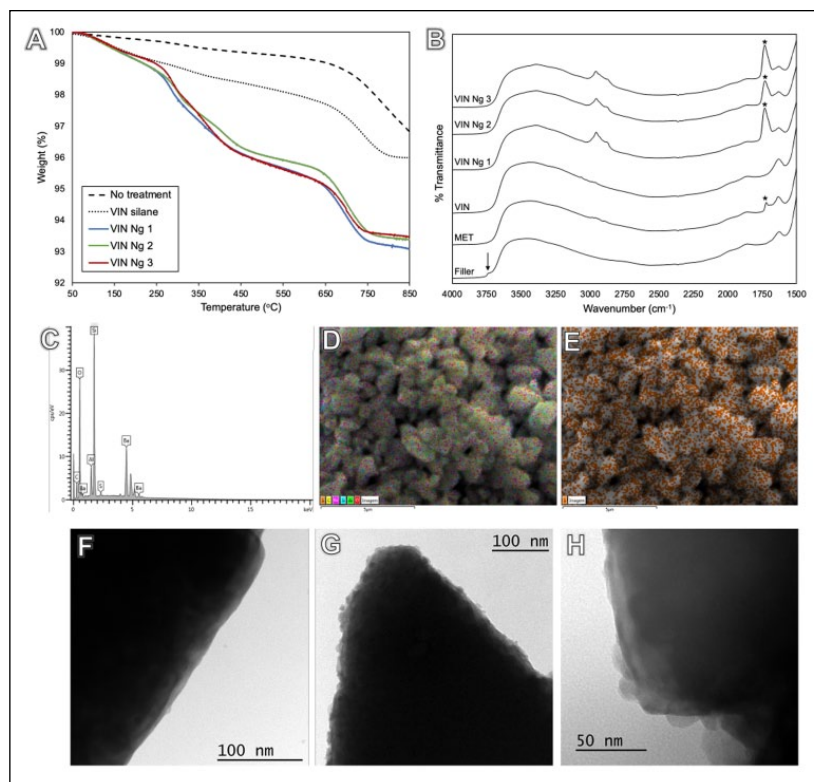tion kinetic data, which were collected for 10 min during and continuing after curing light exposure. Polymerization rate (R_{Pmax}) was calculated as the maximum in the first derivative of the conversion versus time curve.

PS (n = 5; 6 mm in diameter and 1-mm-thick disc specimen) was evaluated with a tensometer (Volpe Research Center, American Dental Association) coupled with Fourier transform near-infrared spectroscopy, as described in the Appendix.

Volumetric shrinkage (VS; n = 5; 6 mm in diameter and 1-mm-thick disc specimen) was evaluated with a noncontact linear variable differential transducer-based linometer (Academic Center for Dentistry Amsterdam), as described in the Appendix.

Viscosity measurements of nanogel resin blends (n = 5) were performed with a cone/plate digital viscometer (CAP 2000; Brookfield). Rheology of the composites (n = 2) was assessed by photorheometry (ARES; TA Instruments) while being photopolymerized at 50 mW/cm^2 (400 to 500 nm; Acticure 4000, EXFO) for 10 min. Detailed rheology testing is described in the Appendix.
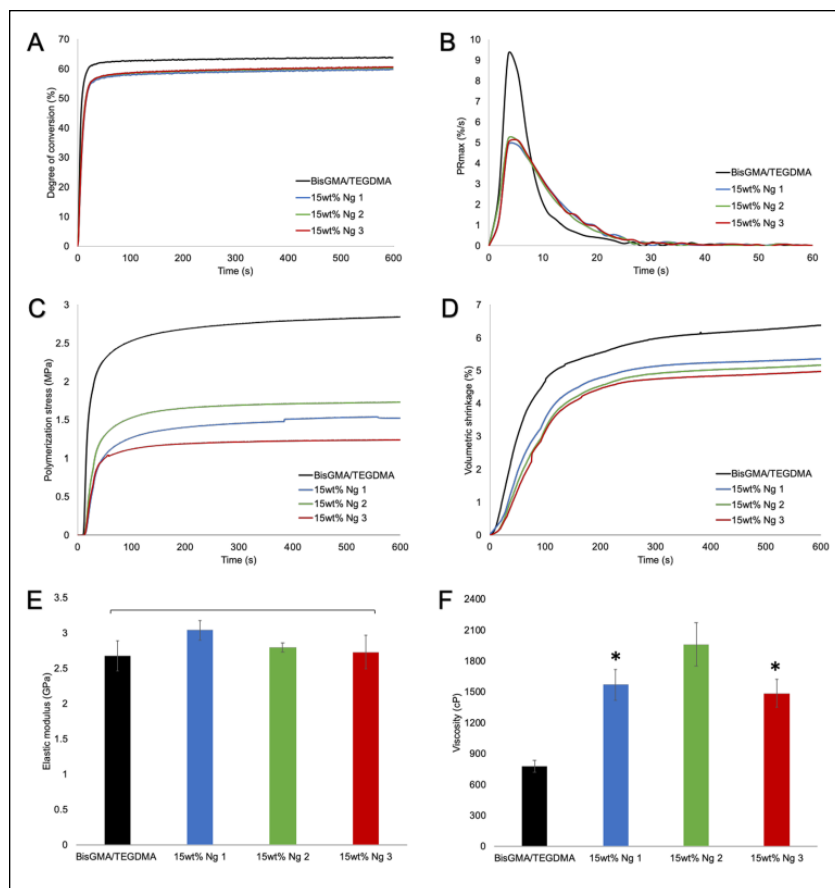
Figure 2. Conversion and property development in nanogel-modified resins. (**A**) Polymerization kinetics of BisGMA/TEGDMA shows slightly diminished degree of conversion when resin is loaded with 15 wt% of nanogels. (**B**) In contrast, the maximum polymerization rate is noticeably lower for nanogel systems. (**C**) The polymerization stress with nanogel loading is approximately half that of the control resin, and (**D**) it accompanies a decrease in volumetric shrinkage as well. (**C**) The smaller, lower Tg nanogel additive tended to provide a greater degree of stress reduction than the larger, higher Tg nanogel analog. (**E**) Notably, the flexural modulus of nanogel-loaded resins is similar to control. (**F**) Incorporation of nanogel increased resin viscosity significantly, especially in the case of the larger Ng 2. (E, F) Values are presented as mean ± SD. *$P < 0.05$. BisGMA/TEGDMA, bisphenol A glycidyl dimethacrylate/triethylene glycol dimethacrylate; Ng, nanogel; Tg, glass transition temperature.

The 3-point bending test (International Organization for Standardization 2009) was used to determine the flexural modulus (FM) and flexural strength (FS) of the materials ($n = 5$; bar specimens of 2 mm × 2 mm × 25 mm) as described in the Appendix.

Statistical Analysis

Normal distribution and equal variance were assessed by Shapiro-Wilk and Brown-Forsythe tests. Data from DC, R_{Pmax}, PS, VS, FM, and FS were evaluated with split-plot 1-way analysis of variance for resin formulations (factor: material, 4 levels) and composites (factor: material, 10 levels). Tukey post hoc tests were applied to detect pairwise mean differences among groups. For all statistical testing, a preset global significance level of 5% was used.

Results

Gel permeation chromatography analysis demonstrated similar molecular weight for nanogels 1 and 3 and a higher molecular weight for Ng 2 with a consequently larger hydrodynamic radius as intended by the reduced chain transfer agent concentration. According to dynamic mechanical analysis, the nanogels presented different Tg's as expected per the different comonomers and reactant ratios selected. Ellman's reagent test assessed slightly higher thiol content for Ng 3 (Table 1) as compared with the other nanogels.

Filler surface treatment was estimated by thermogravimetric analysis as 1 wt% for silane and an additional 3 ± 1 wt% for nanogels (Fig. 1A). The amount of nanogel covalently added to the filler surface was optimized by varying the reaction time to provide an appropriate nanogel content to modulate stress development without decreasing FM (Appendix Fig. 3). Diffuse reflectance Fourier transform infrared spectroscopy (Fig. 1B) showed the presence of methacrylate carbonyl peak (1,706 cm^{-1}) and multiple aliphatic peaks (2,856 to 2,962 cm^{-1}) for nanogel-based surface treatments. Energy-dispersive x-ray analysis identified C, O, Al, Si, and Ba in the composition of the silanated fillers. S correspondent to thiol functional groups was present in nanogel-modified fillers (Fig. 2C, D; Appendix Table 1). Elemental mapping demonstrated a uniform surface distribution of S on the fillers (Fig. 2E; Appendix Table 2 and Fig. 4). Nanogel attachment to the filler surface was further confirmed with transmission electron microscopy images (Fig. 2F), which indicated nanogels both isolated and in agglomerates on filler surfaces (Fig. 2G, H).

Properties of resins and composites are presented in Table 2. Resins without any glass filler but with 15 wt% free nanogel loading demonstrated significantly lower PS and VS, in which the smaller and lower Tg nanogels generated greater PS reduction (Fig. 2C, D). R_{Pmax} and DC were also significantly decreased for these systems (Fig. 2A, B). Nonetheless, the slightly lower DC did not affect the FM (Fig. 2E), but FS was found to be significantly higher for Ng 1 in comparison with the others. A significant increase in resin viscosity ($P < 0.001$) was found with nanogel addition, in which the nanogels of larger size and higher Tg had the more pronounced effect (Fig. 2F).

When MPS-silanated fillers were associated with free nanogel loaded into the resin phase, the composites demonstrated a compressed range of PS reduction, with all nanogels yielding

Table 2. Properties of Resins and Composites with Different Nanogels.

	DC, %	$R_{Pmax,}$ %/s	PS, MPa	VS, %	FM, GPa	FS, MPa
			Resin			
One-way ANOVA, *P* value	<0.001	<0.001	<0.001	<0.001	0.056	0.010
Control resin	63.9 (0.4)[a]	9.4 (0.2)[a]	2.8 (0.1) [a]	6.4 (0.5)[a]	2.7 (0.2)	121.7 (3.6)[a,b]
Ng 1	59.8 (0.2)[c]	5.1 (0.1)[b]	1.5 (0.2) [b,c]	5.3 (0.2)[b]	3.0 (0.1)	129.4 (1.0)[a]
Ng 2	60.3 (0.3)[b,c]	5.5 (0.1)[b]	1.7 (0.1) [b]	5.2 (0.3)[b]	2.8 (0.1)	118.1 (4.7)[b]
Ng 3	60.7 (0.1)[b]	5.4 (0.3)[b]	1.2 (0.3) [c]	5.0 (0.2)[b]	2.7 (0.2)	118.7 (6.0)[b]
			Composite			
One-way ANOVA, *P* value	<0.001	<0.001	<0.001	<0.001	0.447	<0.001
Control MPS	64.6 (0.4)[a]	10.9 (0.4)[a]	2.2 (0.1)[a]	4.3 (0.2)[a]	6.3 (0.3)	145.7 (8.7)[a]
MPS + Ng 1	60.4 (0.4)[b,c]	8.7 (0.2)[b,c]	1.7 (0.1)[b]	3.4 (0.1)[b]	6.2 (0.2)	141.5 (10.6)[a]
MPS + Ng 2	60.2 (0.8)[c]	8.2 (0.3)[c]	1.7 (0.1)[b]	3.3 (0.1)[b]	6.2 (0.1)	132.2 (3.9)[a,b]
MPS + Ng 3	60.3 (1.5)[c]	7.8 (0.1)[c]	1.8 (0.1)[b]	3.1 (0.1)[b]	6.0 (0.1)	126.2 (6.2)[a,b,c]
VIN Ng 1	62.6 (1.1)[a,b]	9.9 (0.6)[a,b]	1.7 (0.1)[b]	4.1 (0.2)[a]	6.0 (0.1)	107.6 (14.2)[b,c]
VIN Ng 2	60.9 (0.3)[b,c]	9.7 (0.2)[a,b]	1.7 (0.1)[b]	4.2 (0.3)[a]	6.4 (0.4)	108.4 (15.2)[b,c]
VIN Ng 3	60.3 (0.9)[c]	9.2 (0.4)[b,c]	1.4 (0.1)[c]	4.0 (0.1)[a]	6.3 (0.3)	112.0 (9.1)[b,c]
VIN Ng 1 + Ng 1	57.3 (0.5)[d]	5.4 (0.3)[d]	1.1 (0.1)[d]	3.1 (0.1)[b]	6.1 (0.2)	102.8 (2.2)[c]
VIN Ng 2 + Ng 2	56.7 (0.3)[d]	6.7 (1.0)[d]	1.2 (0.1)[d]	3.1 (0.2)[b]	6.2 (0.2)	95.8 (6.5)[c]
VIN Ng 3 + Ng 3	61.0 (0.1)[b,c]	7.8 (0.5)[c]	1.2 (0.1)[d]	3.0 (0.2)[b]	6.2 (0.2)	94.1 (8.6)[c]

Within a column, means followed by the same letter are not statistically different ($P > 0.05$). Data presented here for DC and R_{Pmax} were obtained from polymerization kinetics testing.
ANOVA, analysis of variance; DC, degree of conversion; FM, flexural modulus; FS, flexural strength; MPS, γ-methacryloxypropyltrimethoxysilane; Ng, nanogel; PS, polymerization stress; R_{Pmax}, maximum polymerization rate; VIN, trimethoxyvinylsilane; VS, volumetric shrinkage.

significant lower PS and VS as compared with the MPS control (Table 2). A control composite with filler treated with the VIN produced a PS value of 2.3 ± 0.1 MPa, similar to the MPS control. As found for the resin systems, here the DC and R_{Pmax} were also significantly reduced but with no consequences in mechanical properties. VIN nanogel-based composites were able to significantly reduce PS in a magnitude similar to free nanogel addition in composites (reduction of ~20%), unlike the lack of significant decrease in VS. Furthermore, there was a significant reduction in DC but not for the R_{Pmax} as compared with the control, with the exception of VIN Ng 3. The FM of nanogel-based filler composites was similar to control; however, the FS was significantly lower.

Finally, the combined nanogel-modified fillers with free nanogel loading in resin produced a significant stress reduction of ~50% relative to the control (Table 2, Fig. 3). There was a significant decrease in VS, DC, and R_{Pmax} as compared with the control composite, while notably, the FM was not compromised. Only the FS was significantly diminished, as was the case with the VIN nanogel composites. When an equivalent portion of filler was replaced by free nanogel at 5 wt%, it still presented similar PS and FM as the MPS control (Appendix Fig. 5). Photorheology (Fig. 3F) shows the real-time modulus evolution during polymerization. The control demonstrated an early-stage increase in modulus as compared with free nanogel addition or nanogel-modified fillers, with later modulus acquirement when both were combined yet with similar final storage modulus.

Discussion

Nanogels with different sizes and Tg's were synthesized from monofunctional monomers and a difunctional crosslinker, with available thiol functionalities to covalently connect with pendant vinyl groups from the silane on the filler surface via thiol-ene reaction (Hoyle and Bowman 2010; Boulden et al. 2011). Remaining residual thiol groups can participate in matrix-phase methacrylate network formation via chain transfer reaction to couple the matrix and filler in the final polymerized composite (Pfeifer et al. 2011). Nanogel-modified fillers engender ~20% magnitude reduction of PS, regardless of the nanogel used (Table 2). Therefore, the first hypothesis of the study was accepted.

Chain transfer reactions involve exchange of an active radical from a propagating polymer chain to create a nanogel-bound thiyl radical that then initiates incipient growth of a new polymer chain (Bacchi et al. 2016). This process completes the chemical connection between nanogel and matrix, and if the nanogel is preattached to the filler particles, it bonds filler and matrix via the hybrid monomer/nanogel interphase since nanogels are readily swollen by monomer (Dailing et al. 2013). It should be noted that chain transfer reactions are chain breaking, which means that polymerization progresses through a radically assisted step-growth reaction rather than chain growth polymerization (Fairbanks et al. 2009). Within this mechanism, due to delayed gelation and vitrification during polymerization (Pfeifer et al. 2011; Bacchi et al. 2018), internal and interfacial stress is effectively reduced in all the nanogel-modified systems (Table 2).

Among nanogels, Ng 3 provided the lowest PS among resin systems and at the composite interphase (Table 2, Fig. 2C) presumably because of its higher thiol concentration (Table 1) and lower Tg as a bulk nanogel that may produce a more compliant domain within the resin or at the filler interface (Charton et al. 2007). This effect is more easily probed in resin systems, in which differences among nanogel characteristics can be assessed due to the reduced material complexity (i.e., no filler). Interestingly, the same magnitude of PS reduction of the
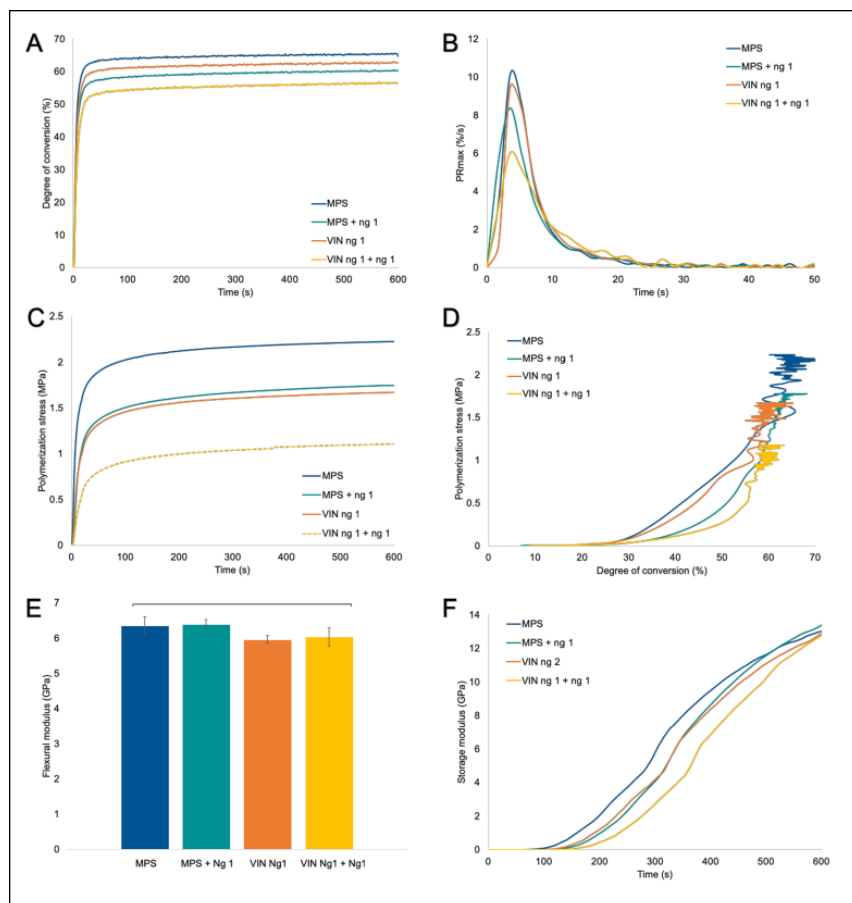
Figure 3. Conversion and property development for composite formulations. (**A**) Real-time polymerization shows a slightly lower degree of conversion for the different composite systems as compared with the MPS control composite, (**B**) while the polymerization rate is slower in systems with free nanogel addition but similar to control for nanogel-based fillers. (**C**) Composite polymerization stress profiles demonstrate a reduction in polymerization stress by about 20% for free nanogel addition and nanogel-based fillers but a 50% reduction when both strategies are combined. (**D**) The MPS control composite and nanogel-based fillers present stress development at lower degrees of conversion than the systems with free nanogel loading. (**E**) The flexural modulus is similar to control for all experimental materials. Real-time elastic modulus development during polymerization shows an early increase in modulus for MPS control, followed by nanogel-based fillers and free nanogel addition with the latest modulus rise observed when both approaches are combined. Values are presented as mean ± SD. (**F**) Notably, the final storage modulus is similar for all groups. MPS, γ-methacryloxypropyltrimethoxysilane; Ng, nanogel; VIN, trimethoxyvinylsilane.

nanogel-based interphases is not observed for similar amounts of nanogel dispersed in the resin (up to 5 wt% vs. 3 ± 1 wt% nanogel attached to the filler, as shown by thermogravimetric analysis in Fig. 1A). Equivalent stress reduction was achieved only with 15 wt% of resin-dispersed nanogel loaded in the composite (Appendix Fig. 5). This likely means that not only did the chain transfer process provide stress relief but it also arose from the interphase itself (Faria et al. 2018). Filler surfaces tethered with monomer-swollen nanogel offer a relatively flexible interphase with relaxation potential to relieve stress during polymerization (Table 2). The compliance of the system is probably activated during polymerization, which assists stress accommodation during the reaction. This is an internalized version of the lower stress observed when external

compliance of a stress measurement device is increased (Meira et al. 2011).

When both strategies of nanogel attached to the filler and dispersed in the resin matrix were combined, a synergic effect was observed, resulting in stress reduction of ~50% (Fig. 3C). Addition of free nanogel to the resin matrix reduced the overall reactive group concentration of BisGMA/TEGDMA, which decreased VS and consequently PS (Table 2; Braga et al. 2005; Moraes et al. 2011). Moreover, simultaneous measurement of real-time conversion and stress development demonstrated a delay to higher conversion for the onset of vitrification for nanogel compositions (Fig. 3D). The R_{Pmax} was also decreased for these systems (Fig. 3B) as expected due to increased viscosity of the resin blend (Fig. 2F; Liu et al. 2012; Liu et al. 2014). A statistically significant decrease in DC was observed for the nanogel-modified materials, with the greatest reduction when both strategies of nanogel introduction are combined. Because DC directly influences VS and elastic modulus, which combine to produce stress (Braga et al. 2005), lower DC values could contribute to diminished PS. However, the marginally lower DC for the experimental materials did not lead to any decrease in FM (Table 2), and as such, small reductions in final conversion of compositionally different materials, absent any modulus reduction, would not be expected to contribute significantly toward lower PS.

There was a substantial reduction in FS for composites with nanogel-modified filler surfaces (Table 2). This effect was not evident when the same nanogels were freely dispersed in the resin phase, which suggests that shortened polymer chains in the vicinity of the critical filler interface due to the chain transfer mechanism may be limiting ultimate strength. A means to probe this question would involve use of methacrylate-functionalized nanogels attached to filler surfaces to allow direct copolymerization between matrix and filler-tethered nanogel interphase. It should be noted that any residual vinyl silane groups on the filler surface can copolymerize with the methacrylate matrix. Indeed, when fillers treated with VIN only were tested without nanogel addition, composite FS was 135.5 ± 6.8 MPa.

Contrary to the FS effects, FM was not compromised for any experimental systems (Table 2). Thereby, the second hypothesis was also accepted. This is important since a PS reduction is usually accompanied by a decrease in elastic modulus (Braga et al. 2005; Stansbury 2012). The modulus retention

indicates that the hybrid matrix/nanogel interphase has an overall crosslink density similar to the BisGMA/TEGDMA control network.

Despite the exciting results, a limitation of this study was the reduction in FS associated with thiol-functional nanogels applied to filler surfaces. Alternative functional silanes on the filler surface with different complementary functionality and reactive sites within the nanogels should be explored further. The interface/interphase design presented here provides a generic approach that can be explored to improve materials while accommodating existing resins and fillers used in dental composites, which facilitates the potential translation into clinical application.

Conclusion

A nanogel-based filler-matrix interphase is able to reduce PS even with minimum amounts of nanogel, which can be combined with free nanogel additives in the resin phase to lower VS and dramatically reduce the overall PS of composites. This was accomplished without compromise to modulus, and we see excellent potential for implementation of this designed interphase approach.

Author Contributions

B.M. Fronza, contributed to conception, design, data acquisition, analysis, and interpretation, drafted the manuscript; I.Y. Rad, P.K. Shah, M.D. Barros, contributed to data acquisition, critically revised the manuscript; M. Giannini, contributed to data analysis and interpretation, critically revised the manuscript; J.W. Stansbury, contributed to conception, design, data analysis, and interpretation, critically revised the manuscript. All authors gave final approval and agree to be accountable for all aspects of the work.

Acknowledgments

ORCID iDs

B.M. Fronza ![ORCID iD] https://orcid.org/0000-0002-8444-3225
P.K. Shah ![ORCID iD] https://orcid.org/0000-0002-5839-1687

References

Bacchi A, Nelson M, Pfeifer CS. 2016. Characterization of methacrylate-based composites containing thio-urethane oligomers. Dent Mater. 32(2):233–239.

Bacchi A, Yih JA, Platta J, Knight J, Pfeifer CS. 2018. Shrinkage/stress reduction and mechanical properties improvement in restorative composites formulated with thio-urethane oligomers. J Mech Behav Biomed Mater. 78:235–240.

Boaro LC, Froes-Salgado NR, Gajewski VE, Bicalho AA, Valdivia AD, Soares CJ, Miranda Junior WG, Braga RR. 2014. Correlation between polymerization stress and interfacial integrity of composites restorations assessed by different in vitro tests. Dent Mater. 30(9):984–992.

Boulden JE, Cramer NB, Schreck KM, Couch CL, Bracho-Troconis C, Stansbury JW, Bowman CN. 2011. Thiol-ene-methacrylate composites as dental restorative materials. Dent Mater. 27(3):267–272.

Braga RR, Ballester RY, Ferracane JL. 2005. Factors involved in the development of polymerization shrinkage stress in resin-composites: a systematic review. Dent Mater. 21(10):962–970.

Braga RR, Koplin C, Yamamoto T, Tyler K, Ferracane JL, Swain MV. 2013. Composite polymerization stress as a function of specimen configuration assessed by crack analysis and finite element analysis. Dent Mater. 29(10):1026–1033.

Charton C, Falk V, Marchal P, Pla F, Colon P. 2007. Influence of Tg, viscosity and chemical structure of monomers on shrinkage stress in light-cured dimethacrylate-based dental resins. Dent Mater. 23(11):1447–1459.

Dailing E, Liu J, Lewis S, Stansbury J. 2013. Nanogels as a basis for network construction. Macromol Symp. 329(1):113–117.

Fairbanks BD, Scott TF, Kloxin CJ, Anseth KS, Bowman CN. 2009. Thiol-yne photopolymerizations: novel mechanism, kinetics, and step-growth formation of highly cross-linked networks. Macromolecules. 42(1):211–217.

Faria ESAL, Dos Santos A, Tang A, Girotto EM, Pfeifer CS. 2018. Effect of thiourethane filler surface functionalization on stress, conversion and mechanical properties of restorative dental composites. Dent Mater. 34(9):1351–1358.

Fronza BM, Rueggeberg FA, Braga RR, Mogilevych B, Soares LE, Martin AA, Ambrosano G, Giannini M. 2015. Monomer conversion, microhardness, internal marginal adaptation, and shrinkage stress of bulk-fill resin composites. Dent Mater. 31(12):1542–1551.

Hoyle CE, Bowman CN. 2010. Thiol-ene click chemistry. Angew Chem Int Ed Engl. 49(9):1540–1573.

Huang S, Podgorski M, Zhang X, Sinha J, Claudino M, Stansbury JW, Bowman CN. 2018. Dental restorative materials based on thiol-Michael photopolymerization. J Dent Res. 97(5):530–536.

International Organization for Standardization. 2009. ISO 4049:2009. Dentistry—polymer-based restorative materials. Geneva (Switzerland): International Organization for Standardization; [accessed 2019 Jan 4]. https://www.iso.org/standard/42898.html.

Jiang Y, Chen J, Deng C, Suuronen EJ, Zhong Z. 2014. Click hydrogels, microgels and nanogels: emerging platforms for drug delivery and tissue engineering. Biomaterials. 35(18):4969–4985.

Liu J, Howard GD, Lewis SH, Barros MD, Stansbury JW. 2012. A study of shrinkage stress reduction and mechanical properties of nanogel-modified resin systems. Eur Polym J. 48(11):1819–1828.

Liu J, Rad IY, Sun F, Stansbury JW. 2014. Photo-reactive nanogel as a means to tune properties during polymer network formation. Polym Chem. 5(1).

Lowe AB. 2010. Thiol-ene "click" reactions and recent applications in polymer and materials synthesis. Polym Chem-Uk. 1(1):17–36.

Meira JB, Braga RR, Ballester RY, Tanaka CB, Versluis A. 2011. Understanding contradictory data in contraction stress tests. J Dent Res. 90(3):365–370.

Moraes RR, Garcia JW, Barros MD, Lewis SH, Pfeifer CS, Liu J, Stansbury JW. 2011. Control of polymerization shrinkage and stress in nanogel-modified monomer and composite materials. Dent Mater. 27(6):509–519.

Nayif MM, Nakajima M, Foxton RM, Tagami J. 2008. Bond strength and ultimate tensile strength of resin composite filled into dentine cavity: effect of bulk and incremental filling technique. J Dent. 36(3):228–234.

Pfeifer CS, Wilson ND, Shelton ZR, Stansbury JW. 2011. Delayed gelation through chain-transfer reactions: mechanism for stress reduction in methacrylate networks. Polymer (Guildf). 52(15):3295–3303.

Shah PK, Stansbury JW. 2014. Role of filler and functional group conversion in the evolution of properties in polymeric dental restoratives. Dent Mater. 30(5):586–593.

Shah PK, Stansbury JW, Bowman CN. 2017. Application of an addition-fragmentation-chain transfer monomer in di(meth)acrylate network formation to reduce polymerization shrinkage stress. Polym Chem. 8(30):4339–4351.

Sideridou ID, Karabela MM. 2009. Effect of the amount of 3-methacyloxypropyltrimethoxysilane coupling agent on physical properties of dental resin nanocomposites. Dent Mater. 25(11):1315–1324.

Soderholm KJ. 1984. Influence of silane treatment and filler fraction on thermal expansion of composite resins. J Dent Res. 63(11):1321–1326.

Stansbury JW. 2012. Dimethacrylate network formation and polymer property evolution as determined by the selection of monomers and curing conditions. Dent Mater. 28(1):13–22.

Wilson KS, Allen AJ, Washburn NR, Antonucci JM. 2007. Interphase effects in dental nanocomposites investigated by small-angle neutron scattering. J Biomed Mater Res A. 81(1):113–123.

Zhang H, Zhai Y, Wang J, Zhai G. 2016. New progress and prospects: the application of nanogel in drug delivery. Mater Sci Eng C Mater Biol Appl. 60:560–568.